CENPE promotes lung adenocarcinoma proliferation and is directly regulated by FOXM1

LINA SHAN[1], MINJIE ZHAO[1], YA LU[1], HONGJUAN NING[1], SHUMAN YANG[2], YONGGUI SONG[3], WENSHU CHAI[1] and XIANBAO SHI[1]

[1]Department of Respiratory, The First Affiliated Hospital of Jinzhou Medical University, Jinzhou, Liaoning 121001; [2]School of Public Health, Jilin University, Changchun, Jilin 130021; [3]School of Pharmacy, Jiangxi University of Traditional Chinese Medicine, Nanchang, Jiangxi 330006, P.R. China

Received December 31, 2018; Accepted May 14, 2019

DOI: 10.3892/ijo.2019.4805

Abstract. Lung cancer is the most common and most lethal type of cancer. A sustained proliferative capacity is one of the hallmarks of cancer, and microtubules serve an important role in maintaining a sustained cell cycle. Therefore, understanding the regulation of microtubule proteins in the cell cycle is important for tumor prevention and treatment. Centromere protein E (CENPE) is a human kinetochore protein that is highly expressed in the G2/M phase of the cell cycle. The present study identified that CENPE is highly expressed in lung adenocarcinoma (LUAD) tissues. Following knockdown of CENPE expression, the proliferation of lung cancer cells was inhibited. In addition, it was revealed that forkhead box M1 (FOXM1) is significantly correlated with CENE expression. Following FOXM1-knockdown, the expression level of CENPE was decreased and the proliferation of lung cancer cells was inhibited. Overexpression of FOXM1 promoted the expression of CENPE and the proliferation of lung cancer cells. A chromatin immunoprecipitation assay identified that FOXM1 binds directly to the promoter region of CENPE. Therefore, the present data demonstrated that CENPE can promote the proliferation of LUAD cells and is directly regulated by FOXM1.

Introduction

Worldwide, there were ~18.1 million new cancer cases and 9.6 million cancer-associated mortalities in 2018 (1). Among all types of cancer, lung cancer has the highest incidence and mortality rates, with 2.1 million new lung cancer cases and 1.8 million mortalities predicted in 2018, which accounts for ~18.4% of all cancer-associated mortalities (1). Non-small cell lung carcinoma (NSCLC) is the most common histological type of lung malignancy. Lung adenocarcinoma (LUAD) accounts for ~50% of all lung cancer cases (2). In the past few decades, clinical trials for the treatment and examination of lung adenocarcinoma have increased, including studies involving chemotherapy, molecular targeted therapy, stereotactic radiotherapy and immunotherapy (3-6). Although NSCLC has been investigated in numerous molecular studies aimed at developing new treatment strategies, the 5-year overall survival rate remains at 4-17%, and 65% of patients with NSCLC are classified as stage III or IV at diagnosis (4,7). Therefore, improved understanding regarding the regulatory mechanisms of NSCLC development and progression is urgently required for the improvement of cancer treatment.

Centrosome protein E (CENPE) is a kinesin-like motor protein that accumulates at the G2 phase of the cell cycle (8). Unlike other centrosome-associated proteins, it is not present during interphase and first appears at the centromere region of chromosomes during prometaphase (9). Therefore, cells with rapid proliferation have higher levels of CENPE expression and CENPE is upregulated in numerous types of solid cancer (10). Certain studies have identified that reducing the expression of CENPE can inhibit cancer cell proliferation. In prostate cancer, genetic deletion or pharmacological inhibition of CENPE was demonstrated to significantly decrease tumor growth (11). In high-grade glioma cells, knockdown of CENPE, kinesin family member 14 or non-SMC condensin I complex subunit G combined with temozolomide-treatment resulted in a combined suppressive effect on cell proliferation (12). In addition, small interfering RNA (siRNA)-induced knockdown of CENPE in human neuroblastoma cell lines can inhibit cellular proliferation (13). Targeting CENPE with the small molecular inhibitor GSK923295 inhibited the in vitro proliferation of 19 neuroblastoma cell lines and delayed tumor growth in three xenograft models (13). Furthermore, one study identified that CENPE can interact

Correspondence to: Professor Xianbao Shi or Professor Wenshu Cai, Department of Respiratory, The First Affiliated Hospital of Jinzhou Medical University, 5 Renmin Street, Guta, Jinzhou, Liaoning 121001, P.R. China
E-mail: sxbsln@163.com
E-mail: cws1964 @163.com

Key words: centromere protein E, forkhead box M1, proliferation, non-small cell lung carcinoma

with FA complementation group A, which may serve an important role in cell cycle control and the pathogenesis of tumor (14).

In summary, previous studies have demonstrated that CENPE is associated with the proliferation of certain cancer cells. However, to the best of our knowledge, the role and regulatory mechanisms of CENPE in NSCLC have not been studied. The present study identified that the expression level of CENPE is higher in LUAD tissues compared with normal tissues. Cell proliferation in the A549 and PC9 cell lines was significantly inhibited following knockdown of CENPE. In addition, it was identified that the expression of CENPE in LUAD is directly regulated by FOXM1.

Materials and methods

Sample collection and cell culture. Between March 2018 and June 2018, seven LUAD tumor samples and seven paired normal lung tissue samples were collected from patients at The First Affiliated Hospital of Jinzhou Medical University (Jinzhou, China). The tumor and normal tissue samples were obtained by lobectomy, and the distance between the tumor tissue and normal lung tissue was ~6 mm. The patients included five males and two females, with a mean age of 56 years (range, 41-78 years). The present study was approved by the Ethics Committee of the First Affiliated Hospital of Jinzhou Medical University and written informed consent was obtained from each individual. The A549 and PC9 human LUAD cell lines were purchased from the American Type Culture Collection (Manassas) and cultured in DMEM high glucose (Gibco; Thermo Fisher Scientific, Inc.) supplemented with 10% fetal bovine serum (FBS; Gibco; Thermo Fisher Scientific, Inc.) and 1% penicillin/streptomycin (Gibco; Thermo Fisher Scientific, Inc.) at 37˚C in a humidified atmosphere containing 5% CO_2.

siRNA and plasmid transfection. A549 or PC9 cells ($5x10^5$/well) were seeded in 6-well plates, cultured overnight and then transfected with 100 nmol/l CENPE siRNA, 100 nmol/l FOXM1 siRNA or 100 nmol/l negative control siRNA using Lipofectamine® 3000 (Invitrogen; Thermo Fisher Scientific, Inc.), according to the manufacturer's protocol. The sequences of the siRNAs were as follows: CENPE, 5'-GGCUGUAAUAUAAAUCGAA-3' (11); FOXM1 5'-GCUCAUACCUGGUACCUAU-3 (15); and negative control, 5'-UUCUCCGAACGUGUCACGU-3' (Shanghai GenePharma, Co., Ltd.).

The FOXM1 expression plasmid and control plasmid were purchased from Guangzhou FulenGen Co., Ltd. (Guangzhou, China) and transfected into A549 cells due to the lower expression of FOXM1 in these cells compared with PC9 cells (16). Transfections were performed in 6-well plates using Lipofectamine® 3000 transfection reagent (Gibco; Thermo Fisher Scientific, Inc.,), according to the manufacturer's protocol. In total, the cells were transfection with 2 μg plasmid/well. Cells were harvested and subjected to analysis 48 h after transfection.

Reverse transcription-quantitative polymerase chain reaction (RT-qPCR). Total RNA was extracted from tissue samples and cells using TRIzol® reagent (Invitrogen; Thermo Fisher Scientific, Inc.). RNA was reverse transcribed into cDNA using the RT reagent kit with gDNA Eraser (Takara Bio, Inc.). The reaction conditions were as follows: 42˚C for 2 min, 37˚C for 15 min and 87˚C for 5 sec. qPCR was performed in a reaction mix with SYBR Green (Takara Bio, Inc.) and was performed in triplicate with an ABI 7500 Prism Sequence Detection system (Applied Biosystems; Thermo Fisher Scientific, Inc.). The following conditions were used: 95˚C for 30 sec for initial denaturation followed by 40 cycles of 95˚C for 5 sec and 60 ˚C for 34 sec. All qPCR primers were purchased from Invitrogen (Invitrogen; Thermo Fisher Scientific, Inc.) and the sequences were as follows: CENPE forward, 5'-GATTCTGCCATACAAGGCTACAA-3' and reverse, 5'-TGCCCTGGGTATAACTCCCAA-3'; FOXM1 forward, 5'-GGAGCAGCGACAGGTTAAGG-3' and reverse, 5'-GTTGATGGCGAATTGTATCATGG-3'; and GAPDH forward, 5'-ACAACTTTGGTATCGTGGAAGG-3' and reverse, 5'-GCCATCACGCCACAGTTTC-3'. Relative expression levels were calculated using the $2^{-\Delta\Delta Cq}$ method (17).

Western blot analysis. Total protein was extracted from the cells or tissue samples using RIPA lysis buffer (Beyotime Institute of Biotechnology) with 1% protease inhibitor phenylmethanesulfonyl fluoride (Beyotime Institute of Biotechnology). The lysates were centrifuged at 1,3000 x g for 15 min at 4˚C and protein concentration was measured using a BCA kit (Beyotime Institute of Biotechnology). Subsequently, 40 μg protein/lane was separated by 10% SDS-PAGE and the proteins were then transferred to a PVDF membrane (Roche Applied Science). The membrane was blocked with 5% BSA (Wuhan Boster Biological Technology, Ltd.) for 1 h at room temperature and then incubated at 4˚C overnight with primary antibodies. Following incubation with appropriate HRP-conjugated secondary antibodies, including goat anti-mouse IgG (cat. no. BA1050; 1:5,000; Wuhan Boster Biological Technology, Ltd.) and goat anti-rabbit IgG (cat. no. BA1054; 1:5,000; Wuhan Boster Biological Technology, Ltd.), for 1 h at room temperature, the membranes were visualized with an ECL kit (Beyotime Institute of Biotechnology) The primary antibodies for western blot analysis included mouse monoclonal anti-GAPDH (1:2,000; cat. no. BM1985; Wuhan Boster Biological Technology, Ltd.), rabbit anti-FOXM1 (1:1,000; cat. no. ab184637; Abcam) and rabbit anti-CENPE (1:1,000; cat. no. ab133583; Abcam).

Cell proliferation assay. Cell Counting Kit-8 (CCK-8; Dojindo Molecular Technologies, Inc.) and 5-ethynyl-2'-deoxyuridine (EdU; GeneCopoeia, Inc.) assays were used to detect proliferation. In the CCK-8 assay, 24 h post-transfection, cells were seeded in a 96-well plate at a density of 3,000 cells/well and cultured overnight at 37˚C in a humidified atmosphere containing 5% CO_2. CCK-8 reagent was then added to the wells and the absorbance at 450 nm was detected following culture for 24, 48 and 72 h at 37˚C.

The iClick™ EdU Andy Fluor™ 647 Flow Cytometry assay kit (GeneCopoeia, Inc.) was used to evaluate cell proliferation in the EdU assay. A total of 24 h post-transfection, A549 and PC9 cells, cultured in DMEM high glucose supplemented with 10% FBS, were treated with EdU (10 μM) for 6 h and the assays were performed according to manufacturer's protocol. The

cells were then analyzed using a flow cytometer and analysis was performed with FlowJo v10 software (FlowJo LLC).

Chromatin immunoprecipitation (ChIP) assay. The FOXM1 binding site on the CENPE promoter region was analyzed using the Cistrome Data Browser (http://cistrome.org/db/#/) (18), with the following parameters: Biological sources; Neuroblastoma cell, Brain; and Factors; FOXM1, SK-N-SH, CENPE (19). The CENPE promoter sequence was obtained from the Eukaryotic Promoter Database (https://epd.epfl.ch/) (20). Subsequently, the binding site was analyzed using the AnimalTFDB3.0 database (http://bioinfo.life.hust.edu.cn/AnimalTFDB/) (21). The following two pairs of primers were used in the present study: Primer 1 (114 bp) forward, 5'-GACGGCAATTCTGTTTGGGT-3' and reverse, 5'-CTGCCAAAAGCTAGCGAACG-3'; and primer 2 (218 bp) forward, 5'-CCCTCTCCTGTTTAGCAGTG-3' and reverse, 5'-CCGCCATCCTATCAGGCTG-3'.

The ChIP assay was performed using the SimpleChIP™ Enzymatic Chromatin IP kit (cat. no. 9003; Cell Signaling Technology, Inc.), according to the manufacturer's protocol. In brief, $4x10^6$ A549 cells were fixed with formaldehyde at room temperature for 15 min and lysed on ice for 5 min using the lysate in the kit, and then chromatin was harvested and fragmented using sonication. Antibodies specific to FOXM1 (1:100; cat. no. ab184637; Abcam) were used to recruit the target DNA overnight at 4˚C and the complex was precipitated by Protein G magnetic beads for 2 h at 4˚C. Normal rabbit IgG (1:300; cat. no. 2729; Cell Signaling Technology, Inc.) was used as the negative control and incubated with the sample overnight at 4˚C, followed by precipitation of the complex with Protein G magnetic beads for 2 h at 4˚C. Following immunoprecipitation, the protein-DNA complex was reversed and the DNA was purified. The enriched DNA was subjected to PCR analysis. PCR was performed with PCR Master mix (cat. no. KT201; Tiangen Biotech, Co., Ltd.), 2 μl DNA, 0.5 μl of each forward and reverse primers, and 7 μl ddH_2O. The reaction conditions were as follows: 95˚C for 4 min, 35 cycles of 95˚C for 1 min, 60˚C for 1 min and 72˚C for 1 min, and a final step of 72˚C for 5 min. The PCR products were screened on 2% agarose gel and signals were detected using enhanced chemiluminescence reagent (Beyotime Institute of Biotechnology), followed by scanning using a FluorChem HD imaging system (ProteinSimple). The following primers were used to detect the co-immunoprecipitated CENPE promoter region by PCR: Primer 1 (114 bp) forward, 5'-GACGGCAATTCTGTTTGGGT-3' and reverse, 5'-CTGCCAAAAGCTAGCGAACG-3'; and primer 2 (218bp) forward, 5'-CCCTCTCCTGTTTAGCAGTG-3' and reverse, 5'-CCGCCATCCTATCAGGCTG-3'.

The Cancer Genome Atlas (TCGA) data analyses. To analyze the differential CENPE/FOXM1 expression levels in normal and LUAD tissues, and the survival of patients with NSCLC the Gene Expression Profiling Interactive Analysis server (http://gepia.cancer-pku.cn/) (22) was used to performed Kaplan-Meier analysis followed by a log-rank test. The CENPE and FOXM1 RNA-sequencing data were downloaded from the cBioPortal (http://www.cbioportal.org/index.do) (23). The expression difference analysis was performed with an unpaired Student's t-test using UALCAN (http://ualcan.path.uab.edu/index.html) (24) and Pearson's correlation analysis was performed using GraphPad Prism 6 software (GraphPad Software, Inc.).

Statistical analysis. Each experiment was independently repeated three times. Statistical analysis was performed with GraphPad Prism 6 software (GraphPad Software, Inc.). All data are presented as the mean ± standard deviation. Data were analyzed using Student's t-test for two groups. $P<0.05$ was considered to indicate a statistically significant difference.

Results

CENPE enhances the proliferation rate of LUAD cells. CCK-8 and EdU assays were used to examine the effect of CENPE on LUAD cell proliferation. The siRNA was designed to knockdown CENPE in A549 and PC9 cells. CENPE mRNA and protein levels were significantly reduced following RNA interference ($P<0.001$; Fig. 1A and B). The EdU assay demonstrated that the proliferation of LUAD cells was inhibited following CENPE-knockdown ($P<0.001$; Fig. 1C and D). The CCK-8 assay demonstrated the same phenomenon ($P<0.01$; Fig. 1E and F).

Expression of CENPE in human LUAD tissues. The expression of CENPE in lung adenocarcinoma and adjacent normal tissues was evaluated by RT-qPCR and western blot analysis. The results demonstrated that the mRNA levels of CENPE in the LUAD tissues were significantly upregulated compared with those in the paired normal tissues ($P<0.01$, Fig. 2A), and similar results were observed following western blot analysis of protein levels (Fig. 2B). Subsequently, the expression of CENPE in TCGA data was analyzed, and the expression level of CENPE was significantly higher in the LUAD samples compared with the normal tissue samples ($P<0.0001$; Fig. 2C). In addition, all tumor grades expressed higher levels of CENPE compared with normal lung tissue and the expression of CENPE was significantly higher in stage II tumors compared with stage I tumors (Fig. 2D). Furthermore, Kaplan-Meier analysis of TCGA data revealed that a lower CENPE expression was associated with improved patient outcomes ($P<0.0001$; Fig. 2E).

CENPE levels are associated with the expression of FOXM1. To further understand the regulatory mechanisms of CENPE, genes associated with CENPE expression were analyzed using TCGA database. It was identified that CENPE expression was highly correlated with transcription factor FOXM1 expression ($r=0.8509$; $P<0.0001$; Fig. 3A). Furthermore, in the tissue samples collected in the present study, the expression levels of FOXM1 and CENPE were significantly correlated ($r=0.7057$; $P<0.0001$; Fig. 3B). In addition, it was identified that FOXM1 expression was significantly higher in LUAD tissues compared with normal tissues ($P<0.05$; Fig. 3C). Analysis of the data from TCGA demonstrated the same result ($P<0.001$; Fig. 3D). All grades of tumors expressed higher levels of FOXM1 compared with normal lung tissue and the expression of CENPE was significantly higher in stage II tumors compared with stage I tumors (Fig. 3E). Additionally,

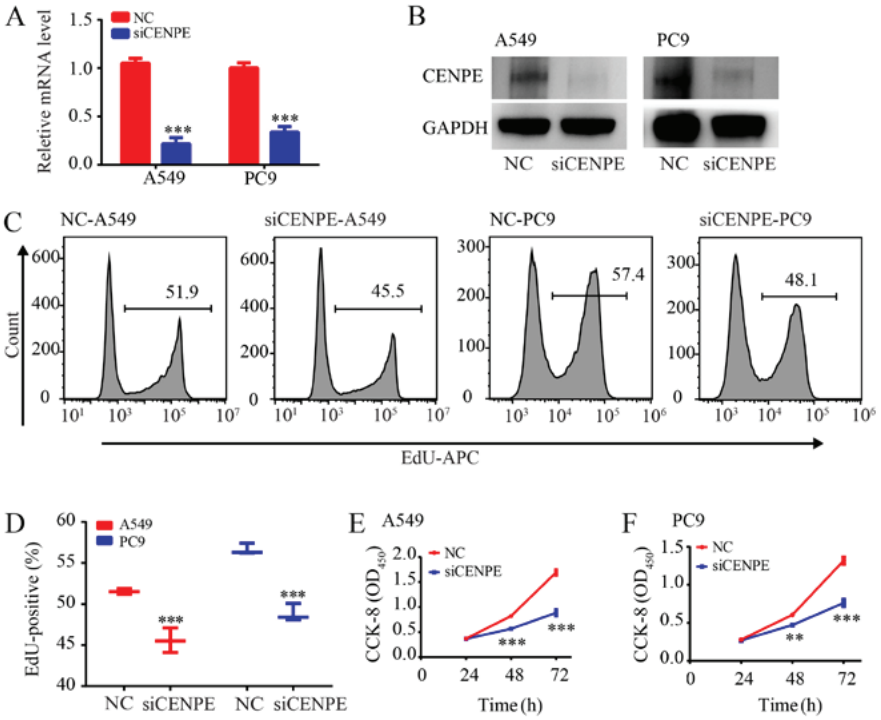

Figure 1. Silencing of CENPE inhibits the proliferation of LUAD cells. (A) Reverse transcription-quantitative polymerase chain reaction analysis of CENPE in A549 and PC9 cells transfected with NC siRNA or siCENPE. (B) Western blot analysis of CENPE in A549 and PC9 cells transfected with control siRNA or siCENPE. (C) Cell proliferation rates as determined by EdU assays in A549 and PC9 cells transfected with control siRNA or siCENPE. (D) Quantification of EdU-positive cells in A549 and PC9 cells transfected with control siRNA or siCENPE. (E) CCK-8 results for the A549 cells. (F) CCK-8 results for the PC9 cells. Experiments were repeated a minimum of three times. Data are presented as the mean ± standard deviation. **P<0.01, ***P<0.001 vs. NC. CENPE, centromere protein E; si, small interfering; EdU, 5-ethynyl-2'-deoxyuridine; CCK-8, Cell Counting Kit-8; NC, negative control; OD, optical density; APC, allophycocyanin.

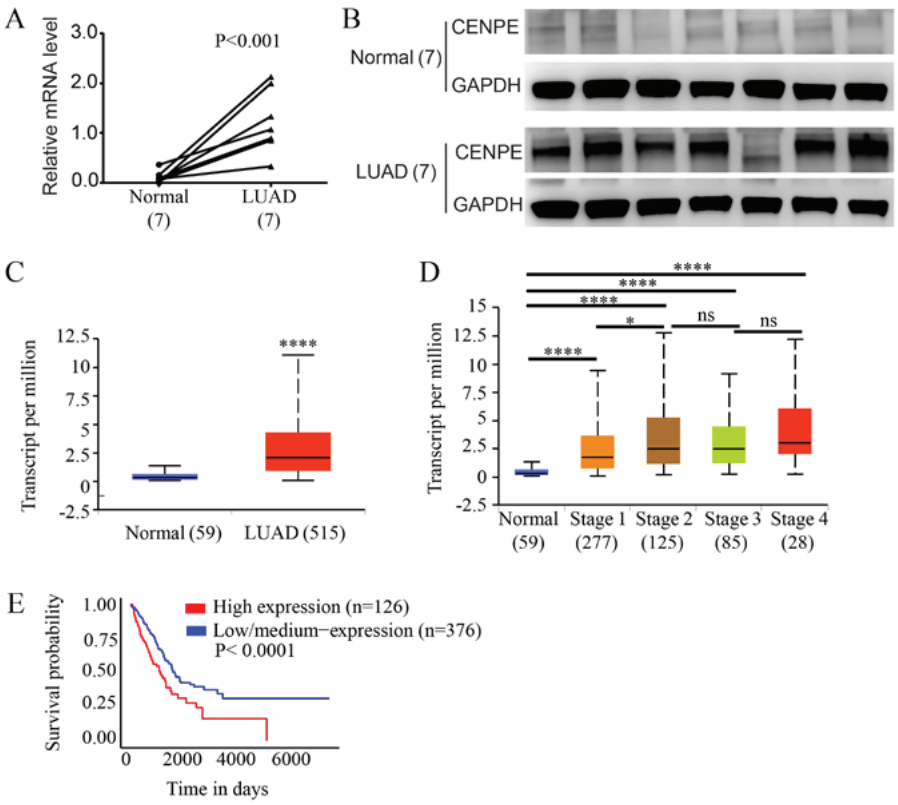

Figure 2. Expression of CENPE in LUAD. (A) Reverse transcription-quantitative polymerase chain reaction analysis of the CENPE expression levels in LUAD and N tissues. (B) Western blot analysis of CENPE expression in LUAD and N tissue. (C) The mRNA levels of CENPE in LUAD and N, according to data from TCGA database. ****P<0.0001 vs. N. (D) CENPE expression based on individual cancer stages, according to data from TCGA database. *P<0.05, ****P<0.0001. (E) Kaplan-Meier analysis of LUAD RNA-sequencing data from TCGA database. CENPE, centromere protein E; LUAD, lung adenocarcinoma; TCGA, The Cancer Genome Atlas; N, normal; ns, not significant.

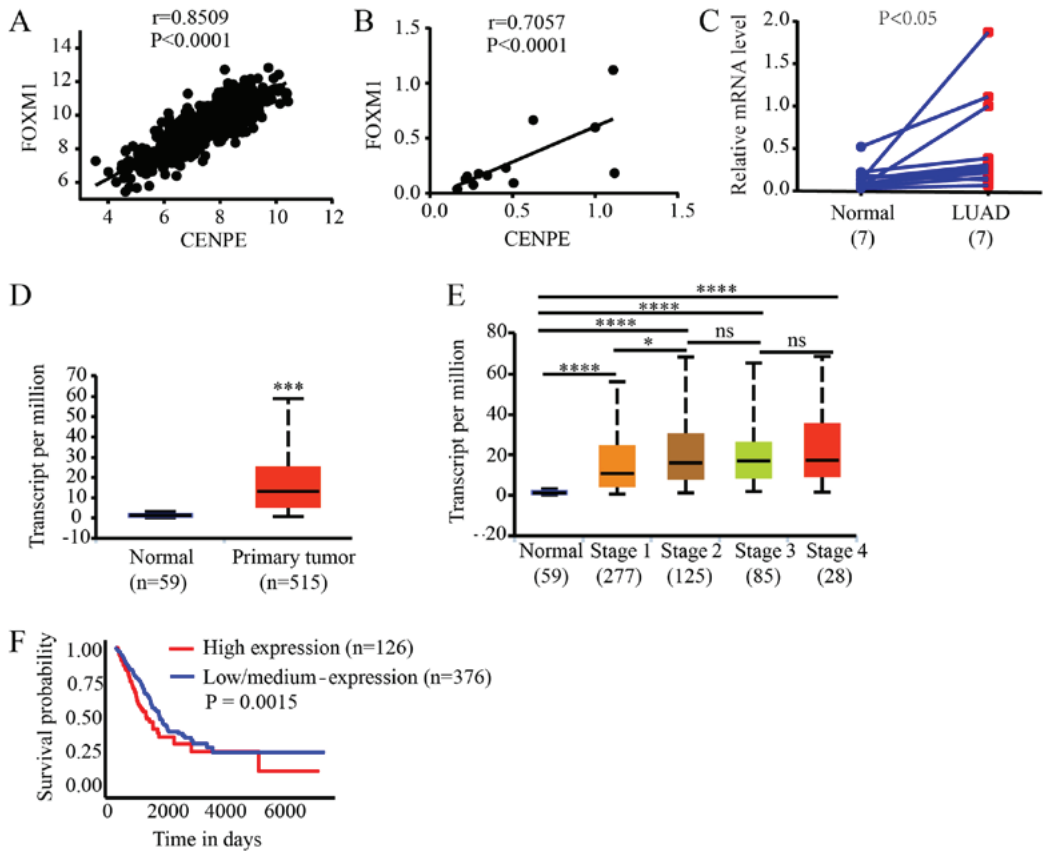

Figure 3. CENPE expression is associated with the expression of FOXM1. (A) Correlation analysis between CENPE and FOXM1 expression in LUAD, according to data from TCGA database. (B) Correlation analysis between CENPE and FOXM1 expression in LUAD, according to data from the patient samples. (C) The mRNA levels of FOXM1 in LUAD and normal tissues, according to data from the patient samples. (D) The mRNA levels of FOXM1 in LUAD and normal tissues, according to data from TCGA database. ***P<0.001. (E) CENPE expression based on individual cancer stages, according to data from TCGA database. *P<0.05, ****P<0.0001. (F) Kaplan-Meier analysis of FOXM1 in the LUAD RNA-sequencing data from TCGA database. CENPE, centromere protein E; LUAD, lung adenocarcinoma; TCGA, The Cancer Genome Atlas; FOXM1, forkhead box M1; ns, not significant.

Kaplan-Meier analysis of TCGA data demonstrated that lower FOXM1 expression was associated with an improved patient outcome (P=0.0015; Fig. 3F).

Silencing of FOXM1 inhibits proliferation of LUAD cells. To verify that FOXM1 regulates the expression of CENPE, siRNAs were designed to knockdown FOXM1 expression in A549 and PC9 cells. It was first demonstrated that FOXM1 was significantly knocked down in both cell lines and CENPE expression was also significantly reduced (P<0.01; Fig. 4A and B). The EdU assay revealed that silencing FOXM1 significantly inhibited the proliferation of LUAD cells (Fig. 4C and D; P<0.01). The CCK-8 assay further demonstrated that knockdown of FOXM1 significantly inhibited the proliferation of LUAD cells (P<0.05; Fig. 4E and F).

Overexpression of FOXM1 promotes proliferation of LUAD cells. To further confirm that FOXM1 regulates CENPE and promotes proliferation of LUAD cells, FOXM1 was overexpressed in A549 cells. RT-qPCR and western blot analysis demonstrated that FOXM1 was significantly overexpressed, and CENPE levels were significantly higher in cells overexpressing FOXM1 (P<0.001; Fig. 5A and B). After FOXM1 was overexpressed, the CCK-8 results revealed a significantly increased proliferation rate (P<0.05; Fig. 5C). Furthermore, the EdU assay demonstrated that overexpression of FOXM1 significantly promoted proliferation of A549 cells (P<0.001; Fig. 5D and E).

CENPE expression is directly regulated by FOXM1. From a previous study, it is understood that transcription factors can bind to the promoter region of genes and directly regulate their transcription (25). Therefore, the present study further analyzed the regulatory mechanism of FOXM1 on CENPE. First, the ChIP-sequencing data of FOXM1 was analyzed using the Cistrome database. The results demonstrated that FOXM1 has a binding peak in the promoter region of CENPE (Fig. 6A). The FOXM1 binding site on the CENPE promoter region (-499 to 100) was then analyzed. It was identified that there are two FOXM1 binding sites in the region of CENPE (Fig. 6B). Primers were then designed using DNA sequences that bind to the peak positions to further validate the conclusions of the binding. The ChIP assay of A549 cells confirmed that the CENPE promoter region contains a binding site for FOXM1 (Fig. 6C). To further confirm this conclusion, the band strengths obtained by CHIP from the control and FOXM1-interference groups were compared, and a lower intensity was observed for the FOXM1-interference group (Fig. 6D). Therefore, the current results indicate that FOXM1 can directly regulate the expression of CENPE in LUAD.

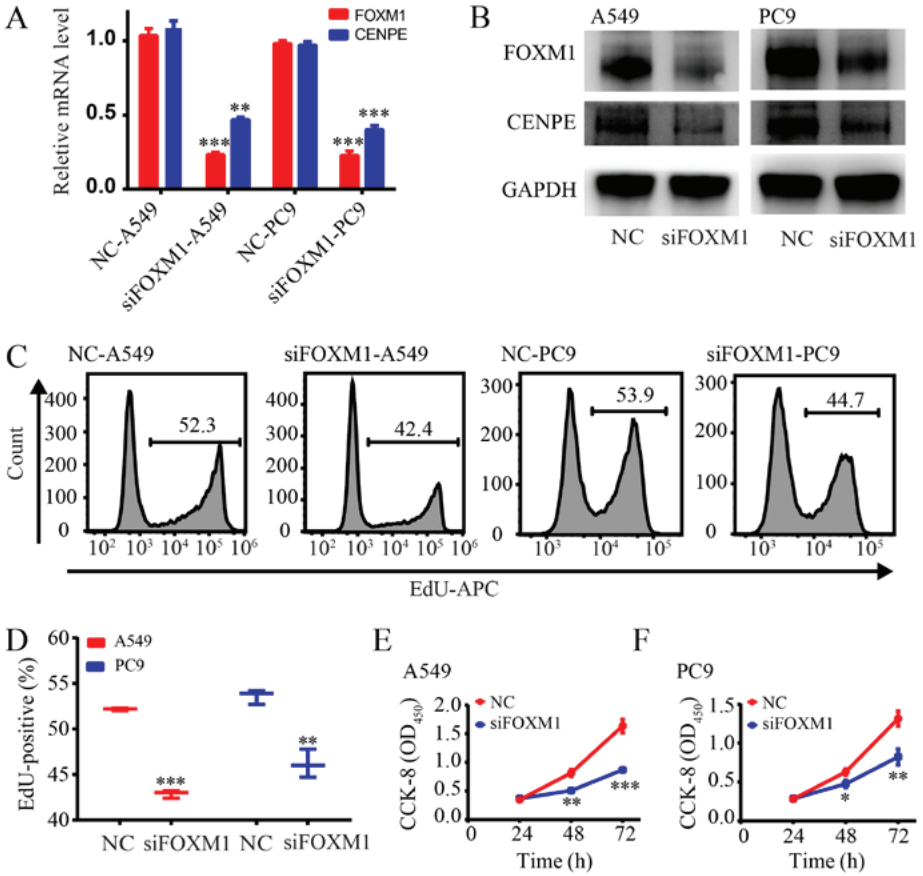

Figure 4. Silencing of FOXM1 inhibits the proliferation of LUAD cells. (A) Reverse transcription-quantitative polymerase chain reaction analysis of CENPE in A549 and PC9 cells transfected with control siRNA or siFOXM1. (B) Western blot analysis of FOXM1 and CENPE in A549 and PC9 cells transfected with control siRNA or siFOXM1. (C) Cell proliferation rates as determined by EdU assays with A549 and PC9 cells. (D) Quantification of EdU-positive A549 and PC9 cells transfected with control siRNA or siFOXM1. (E) CCK-8 results for the A549 group. (F) CCK-8 results for the PC9 group. *P<0.05, **P<0.01, ***P<0.001 vs NC. FOXM1, forkhead box M1; LUAD, lung adenocarcinoma; CENPE, centromere protein E; si, small interfering; NC, negative control; CCK-8, Cell Counting Kit-8; OD, optical density; APC, allophycocyanin; EdU, 5-ethynyl-2'-deoxyuridine.

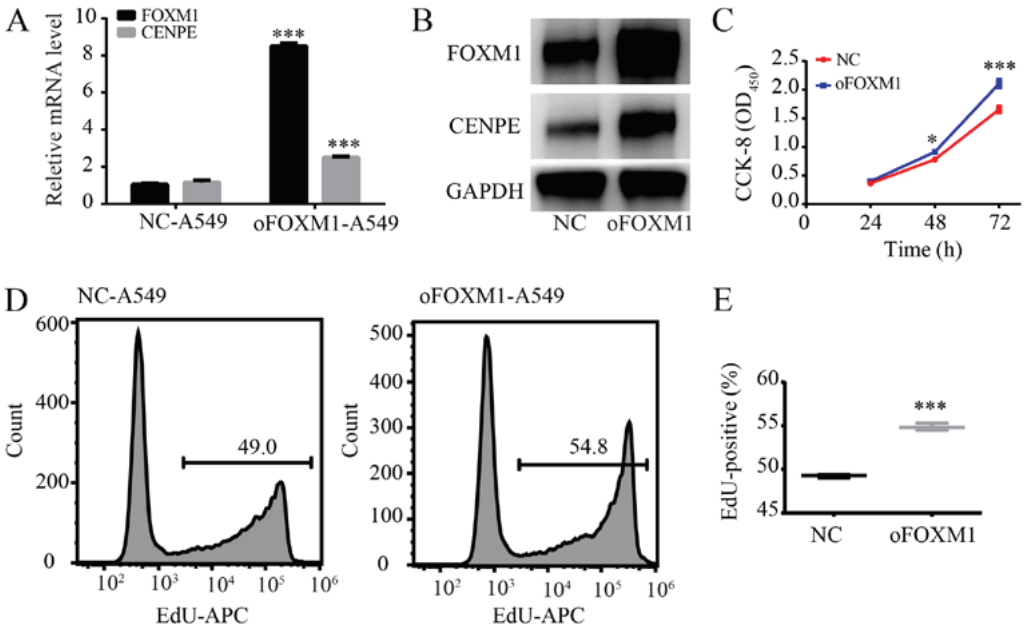

Figure 5. Overexpression of FOXM1 promotes proliferation of A549 cells. (A) Reverse transcription-quantitative polymerase chain reaction analysis of CENPE and FOXM1 in A549 cells transfected with control vector or oFOXM1 vector. (B) Western blot analysis of CENPE and FOXM1 in A549 cells transfected with control vector or oFOXM1 vector. (C) CCK-8 assay results demonstrating that overexpression of FOXM1 promoted proliferation of A549 cells. (D) Cell proliferation rates as determined by EdU assays with A549 cells. (E) Quantification of EdU-positive A549 cells transfected with control vector or oFOXM1 vector. *P<0.05, ***P<0.001 vs. NC. FOXM1, forkhead box M1; CENPE, centromere protein E; si, small interfering; NC, negative control; CCK-8, Cell Counting Kit-8; OD, optical density; APC, allophycocyanin; oFOXM1, forkhead box M1-overexpression; EdU, EdU, 5-ethynyl-2'-deoxyuridine.

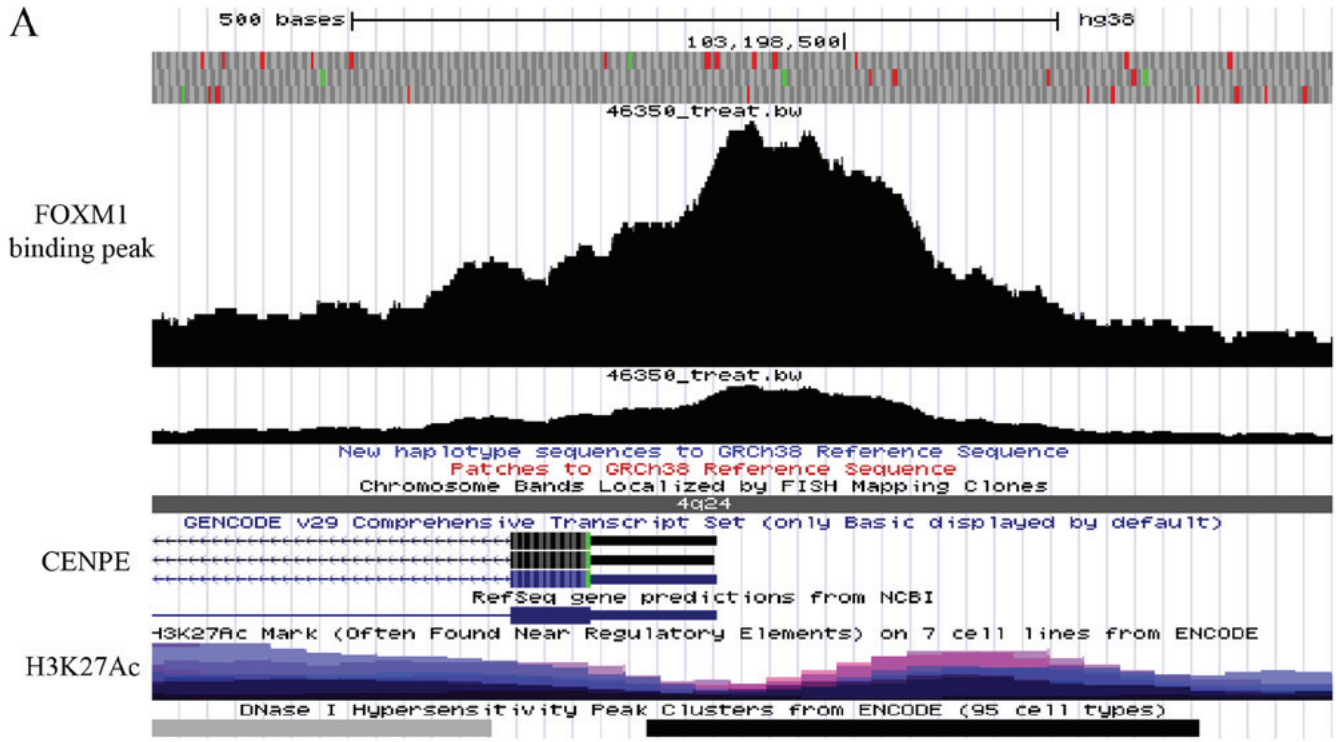

B

>FP007255 CENPE_1 :+U EU:NC; range -499 to 100.

GCGCACAACAGGCTTGTCACGTTTCTGGACTGGACAGCGAATTTCAACTCTTGCTGTTGAAAGTTTATTTTAAA

CTGTTGGTGCAGTTTCTTTAAAAGACGGCAATTCTGTTTGGGTAGTGAAAAATACATGTATCTCTACCTAGTTT

CGTCTACAGGTTCCAAACTTTTTAAGGATGGGGTGGAGGATGACGTTCGCTAGCTTTTGGCAGATAATAGTATT

CTGGTATTCCAGGACCACCACTCTCTGCCCACTCCTGGGAGCCCCTCCCTTCGGCCCTCTCCTCCGACTCTCTG

CTGGGCCCTTTAAATCCCCTCTCCTGTTTAGCAGTGGTCACGCCGCCCGCCTTGCGTCCCCCGCGCTGCTCCGC

ACGTGGAATGGCCCATGACGTCACGAGGCCACGGCTCAATCAGATGCGGCGTTTGGGAAATTTTAAATTTAAAG

GCGGGGCGGCCTGTGAGCCCTGAAGTGCCGGCCGCGGAGGGTCCTGGCCATTTTCCTGGGACCAGTTCAGCCTG

ATAGGATGGCGGAGGAAGGAGCCGTGGCCGTCTGCGTGCGAGTGCGGCCGCTGAACAGCAGGTAGGGGGGCCAC

ACCACGGC

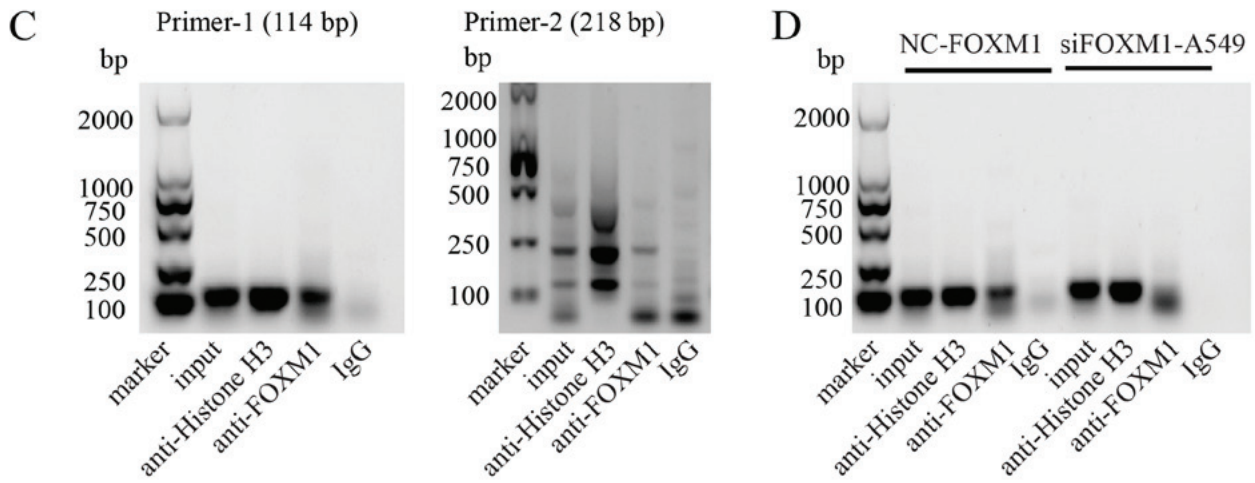

Figure 6. CENPE expression is directly regulated by FOXM1. (A) The FOXM1 binding site on the CENPE promoter region. (B) Prediction of FOXM1 binding sites on the CENPE promoter region (-499 to 100). Red is the predicted binding site. The first pair of primer amplification regions, and the double underline is the second pair of primer amplification regions. (C) Chromatin fragments from A549 cells were immunoprecipitated with antibodies specific to histone H3 (positive control), mouse IgG (NC) and FOXM1. Input, 2% total DNA. The assays demonstrated that FOXM1 binds to the CENPE promoter. (D) The immunoprecipitated DNA of A549 cells expressing NC and siFOXM1 was amplified by polymerase chain reaction and resolved on 1% agarose gels. FOXM1, forkhead box M1; CENPE, centromere protein E; si, small interfering; oFOXM1, forkhead box M1-overexpression; NC, negative control.

Discussion

Mitosis is a key event of the cell cycle. The ability to maintain proliferation is a hallmark of cancer and microtubules serve an important part in maintaining a sustained cell cycle (9). At the same time, numerous microtubule-associated proteins are highly expressed in tumor tissues (9), and targeting microtubule-associated proteins is one way to treat tumors (26). Therefore, further understanding of the regulatory mechanisms of microtubule-associated proteins in lung cancer may improve understanding regarding the cell cycle and also provide new targets for the treatment of tumors. CENPE is a microtubule-associated protein that is highly expressed in numerous types of cancer, including prostate cancer (11) and glioma (27). The present study identified a high expression of CENPE in LUAD tissues and CENPE-knockdown was demonstrated to inhibit the proliferation of LUAD cell lines.

Firstly, the current study identified that CENPE is highly expressed in lung adenocarcinoma using TCGA database, and in grade I and II lung adenocarcinoma the expression was revealed to increase with increasing grade. Subsequently, it was demonstrated that the proliferation of A549 and PC9 cells was inhibited following CENPE-knockdown, indicating that CENPE is associated with the proliferation rate of lung adenocarcinoma. Therefore, CENPE may be a marker of the proliferation rate of a tumor. In other tumor types, there are reports that CENPE can be used as a marker for tumor proliferation. In prolactin pituitary tumors, it was identified that seven genes, including ADAM metallopeptidase with thrombospondin type 1 motif 6 (ADAMTS6), collapsing response mediator protein 1 (CRMP1), pituitary tumor transforming gene, aspartokinase (ASK), cyclin B1 (CCNB1), aurora kinase B and CENPE, were associated with tumor recurrence or progression, and five of these genes (ADAMTS6, CRMP1, ASK, CCNB1 and CENPE) were also associated with the pathological classification (28). In glioma, RNA levels of eight major mitotic spindle assembly checkpoint genes, including CENPE, have been reported to be significantly associated with glioma grade and survival time (27). In invasive ductal carcinoma, CENPE was identified to be one of the top ten potential crucial genes (29). In addition, studies have identified that the expression of CENPE is associated with drug tolerance (30-32). In paclitaxel-resistant ovarian cell lines, it was revealed that CENPE expression is lower (31).

Following bioinformatics analysis, the present study identified that CENPE has a significant correlation with FOXM1 expression, and FOXM1 is also highly expressed in lung adenocarcinoma. In addition, the overall survival rate of patients with high expression of FOXM1 was worse; however, there was a difference between the survival trend of FOXM1 and the survival trend of CENPE. FOXM1 is a transcription factor that participates in all stages of tumor development, predominantly through control of the cell cycle and proliferation, regulating the expression of genes involved in the G1/S and G2/M transitions and M phase progression (33). The forkhead box O3 and FOXM1 transcription factors, functioning downstream of the essential PI3K-Akt, Ras-ERK and JNK/p38MAPK signaling cascades, are crucial for cell proliferation, differentiation, cell survival, senescence, DNA damage repair and cell cycle control (34). Therefore, numerous studies have identified that FOXM1 can promote the proliferation of a number of types of tumor. It has been reported that DEP domain containing 1, negatively regulated by microRNA (miR)-26b, promotes cell proliferation and tumor growth by upregulating FOXM1 expression, indicating an important underlying mechanism of regulating the progression of triple negative breast cancer (35). G2 and S phase-expressed-1 contributes to cell proliferation, migration and invasion by regulating the p53/forkhead box 1 (FOXM1)/CCNB1 pathway and predicts poor prognosis in bladder cancer (36). In U2OS cells, enforced expression of FOXM1 suppressed diallyl disulfide-induced antiproliferation and anti-invasion (37). In glioblastoma cells, miR-876-5p may inhibit the development of glioblastoma by directly targeting FOXM1 (38). In ovarian cancer, hsa_circ_0061140 has been demonstrated to promote cell growth and metastasis through regulation of the miR-370/FOXM1 pathway, mediating the epithelial-mesenchymal transition (39). In ovarian cancer cells, FOXM1 transcriptionally activated PCNA-associated factor to drive cell proliferation (40). In meningioma, the FOXM1/Wnt signaling axis is associated with a mitotic gene expression program, poor clinical outcomes and proliferation (41). In colorectal cancer, one study reported that FOXM1 is critical for the proliferation and growth of colorectal cancer (42). In summary, the aforementioned studies suggest that the expression of FOXM1 is associated with proliferation and mainly regulates the G2/M phase. Therefore, the present study hypothesized that the expression of CENPE may be regulated by FOXM1. Through interference, overexpression and ChIP experiments, it was demonstrated that CENPE can be directly regulated by FOXM1.

In conclusion, the current study revealed that CENPE is highly expressed in LUAD tissues. In addition, FOXM1 is correlated with the expression of CENE and is associated with the proliferation of lung cancer cells. The ChIP assay demonstrated that FOXM1 binds directly to the promoter region of CENPE. Therefore, the current data indicate that CENPE can promote the proliferation of LUAD cells and is directly regulated by FOXM1. In the future it will be important to further understand the signaling pathways that regulate CENPE expression, and the mechanism by which CENPE regulates the cell cycle. In addition, more studies should investigate centromere-associated proteins that are abnormally expressed in tumors. The study of more centromere-associated proteins may provide new targets and a theoretical basis for targeted therapy of cell cycle-associated proteins.

Acknowledgements

The authors would like to thank Dr Gang Zhang (State Key Laboratory of Bioactive Substances and Function of Natural Medicine, Peking Union Medical College and Chinese Academy of Medical Science, Beijing, China) for editing a draft of the manuscript.

Funding

The present study was supported by the National Natural Science Foundation of China (grant no. 81700050).

Availability of data and materials

All data generated or analyzed during this study are included in this published article.

Authors' contributions

XS and WC contributed to the experiment design, drafted the manuscript and performed data analysis. LS conceived or designed the experiments, performed the experiments, wrote the manuscript and performed data analysis. MZ designed the experiments. YL, HN and YS performed the experiments. SY analyzed the data. All authors read and approved the final manuscript.

Ethics approval and consent to participate

The experiments were approved by the Ethics Committee of The First Affiliated Hospital of Jinzhou Medical University (Jinzhou, China) and written informed consent was obtained from each individual.

Patient consent for publication

Not applicable.

Competing interests

The authors declare that they have no competing interests.

References

1. Bray F, Ferlay J, Soerjomataram I, Siegel RL, Torre LA and Jemal A: Global cancer statistics 2018: GLOBOCAN estimates of incidence and mortality worldwide for 36 cancers in 185 countries. CA Cancer J Clin 68: 394-424, 2018.
2. Herbst RS, Heymach JV and Lippman SM: Lung cancer. N Engl J Med 359: 1367-1380, 2008.
3. Herbst RS, Morgensztern D and Boshoff C: The biology and management of non-small cell lung cancer. Nature 553: 446-454, 2018.
4. Hirsch FR, Scagliotti GV, Mulshine JL, Kwon R, Curran WJ Jr, Wu YL and Paz-Ares L: Lung cancer: Current therapies and new targeted treatments. Lancet 389: 299-311, 2017.
5. Mathew M, Enzler T, Shu CA and Rizvi NA: Combining chemotherapy with PD-1 blockade in NSCLC. Pharmacol Ther 186: 130-137, 2018.
6. Rotow J and Bivona TG: Understanding and targeting resistance mechanisms in NSCLC. Nat Rev Cancer 17: 637-658, 2017.
7. Bradbury P, Sivajohanathan D, Chan A, Kulkarni S, Ung Y and Ellis PM: Postoperative adjuvant systemic therapy in completely resected non-small-cell lung cancer: A systematic review. Clin Lung Cancer 18: 259-273 e258, 2017.
8. Testa JR, Zhou JY, Bell DW and Yen TJ: Chromosomal localization of the genes encoding the kinetochore proteins CENPE and CENPF to human chromosomes 4q24-->q25 and 1q32-->q41, respectively, by fluorescence in situ hybridization. Genomics 23: 691-693, 1994.
9. Rath O and Kozielski F: Kinesins and cancer. Nat Rev Cancer 12: 527-539, 2012.
10. Hitti E, Bakheet T, Al-Souhibani N, Moghrabi W, Al-Yahya S, Al-Ghamdi M, Al-Saif M, Shoukri MM, Lánczky A, Grépin R, *et al*: Systematic analysis of AU-rich element expression in cancer reveals common functional clusters regulated by key RNA-binding proteins. Cancer Res 76: 4068-4080, 2016.
11. Liang Y, Ahmed M, Guo H, Soares F, Hua JT, Gao S, Lu C, Poon C, Han W, Langstein J, *et al*: LSD1-mediated epigenetic reprogramming drives CENPE expression and prostate cancer progression. Cancer Res 77: 5479-5490, 2017.
12. Liang ML, Hsieh TH, Ng KH, Tsai YN, Tsai CF, Chao ME, Liu DJ, Chu SS, Chen W, Liu YR, *et al*: Downregulation of miR-137 and miR-6500-3p promotes cell proliferation in pediatric high-grade gliomas. Oncotarget 7: 19723-19737, 2016.
13. Balamuth NJ, Wood A, Wang Q, Jagannathan J, Mayes P, Zhang Z, Chen Z, Rappaport E, Courtright J, Pawel B, *et al*: Serial transcriptome analysis and cross-species integration identifies centromere-associated protein E as a novel neuroblastoma target. Cancer Res 70: 2749-2758, 2010.
14. Du J, Chen L and Shen J: Identification of FANCA as a protein interacting with centromere-associated protein E. Acta Biochim Biophys Sin (Shanghai) 41: 816-821, 2009.
15. Hasson SA, Kane LA, Yamano K, Huang CH, Sliter DA, Buehler E, Wang C, Heman-Ackah SM, Hessa T, Guha R, *et al*: High-content genome-wide RNAi screens identify regulators of parkin upstream of mitophagy. Nature 504: 291-295, 2013.
16. Cancer Cell Line Encyclopedia Consortium; Genomics of Drug Sensitivity in Cancer Consortium: Pharmacogenomic agreement between two cancer cell line data sets. Nature 528: 84-87, 2015.
17. Livak KJ and Schmittgen TD: Analysis of relative gene expression data using real-time quantitative PCR and the 2(-Delta Delta C(T)) Method. Methods 25: 402-408, 2001.
18. Zheng R, Wan C, Mei S, Qin Q, Wu Q, Sun H, Chen CH, Brown M, Zhang X, Meyer CA, *et al*: Cistrome Data Browser: Expanded datasets and new tools for gene regulatory analysis. Nucleic Acids Res 47 (D1): D729-D735, 2019.
19. Gertz J, Savic D, Varley KE, Partridge EC, Safi A, Jain P, Cooper GM, Reddy TE, Crawford GE and Myers RM: Distinct properties of cell-type-specific and shared transcription factor binding sites. Mol Cell 52: 25-36, 2013.
20. Dreos R, Ambrosini G, Groux R, Cavin Périer R and Bucher P: The eukaryotic promoter database in its 30th year: Focus on non-vertebrate organisms. Nucleic Acids Res 45 (D1): D51-D55, 2017.
21. Hu H, Miao YR, Jia LH, Yu QY, Zhang Q and Guo AY: AnimalTFDB 3.0: A comprehensive resource for annotation and prediction of animal transcription factors. Nucleic Acids Res 47 (D1): D33-D38, 2019.
22. Tang Z, Li C, Kang B, Gao G, Li C and Zhang Z: GEPIA: A web server for cancer and normal gene expression profiling and interactive analyses. Nucleic Acids Res 45 (W1): W98-W102, 2017.
23. Gao J, Aksoy BA, Dogrusoz U, Dresdner G, Gross B, Sumer SO, Sun Y, Jacobsen A, Sinha R, Larsson E, *et al*: Integrative analysis of complex cancer genomics and clinical profiles using the cBioPortal. Sci Signal 6: pl1, 2013.
24. Chandrashekar DS, Bashel B, Balasubramanya SAH, Creighton CJ, Ponce-Rodriguez I, Chakravarthi BVSK and Varambally S: UALCAN: A portal for facilitating tumor subgroup gene expression and survival analyses. Neoplasia 19: 649-658, 2017.
25. Lambert SA, Jolma A, Campitelli LF, Das PK, Yin Y, Albu M, Chen X, Taipale J, Hughes TR and Weirauch MT: The human transcription factors. Cell 172: 650-665, 2018.
26. Casaluce F, Sgambato A, Maione P, Ciardiello F and Gridelli C: Emerging mitotic inhibitors for non-small cell carcinoma. Expert Opin Emerg Drugs 18: 97-107, 2013.
27. Bie L, Zhao G, Cheng P, Rondeau G, Porwollik S, Ju Y, Xia XQ and McClelland M: The accuracy of survival time prediction for patients with glioma is improved by measuring mitotic spindle checkpoint gene expression. PLoS One 6: e25631, 2011.
28. He M, Agbu S and Anderson KV: Microtubule motors drive hedgehog signaling in primary cilia. Trends Cell Biol 27: 110-125, 2017.
29. Li C, Luo L, Wei S and Wang X: Identification of the potential crucial genes in invasive ductal carcinoma using bioinformatics analysis. Oncotarget 9: 6800-6813, 2017.
30. Nara M, Teshima K, Watanabe A, Ito M, Iwamoto K, Kitabayashi A, Kume M, Hatano Y, Takahashi N, Iida S, *et al*: Bortezomib reduces the tumorigenicity of multiple myeloma via downregulation of upregulated targets in clonogenic side population cells. PLoS One 8: e56954, 2013.
31. Chong T, Sarac A, Yao CQ, Liao L, Lyttle N, Boutros PC, Bartlett JMS and Spears M: Deregulation of the spindle assembly checkpoint is associated with paclitaxel resistance in ovarian cancer. J Ovarian Res 11: 27, 2018.
32. Horning AM, Wang Y, Lin CK, Louie AD, Jadhav RR, Hung CN, Wang CM, Lin CL, Kirma NB, Liss MA, *et al*: Single-cell RNA-seq reveals a subpopulation of prostate cancer cells with enhanced cell-cycle-related transcription and attenuated androgen response. Cancer Res 78: 853-864, 2018.

33. Liao GB, Li XZ, Zeng S, Liu C, Yang SM, Yang L, Hu CJ and Bai JY: Regulation of the master regulator FOXM1 in cancer. Cell Commun Signal 16: 57, 2018.
34. Yao S, Fan LY and Lam EW: The FOXO3-FOXM1 axis: A key cancer drug target and a modulator of cancer drug resistance. Semin Cancer Biol 50: 77-89, 2018.
35. Zhang L, Du Y, Xu S, Jiang Y, Yuan C, Zhou L, Ma X, Bai Y, Lu J and Ma J: DEPDC1, negatively regulated by miR-26b, facilitates cell proliferation via the up-regulation of FOXM1 expression in TNBC. Cancer Lett 442: 242-251, 2019.
36. Liu A, Zeng S, Lu X, Xiong Q, Xue Y, Tong L, Xu W, Sun Y, Zhang Z and Xu C: Overexpression of G2 and S phase-expressed-1 contributes to cell proliferation, migration, and invasion via regulating p53/FoxM1/CCNB1 pathway and predicts poor prognosis in bladder cancer. Int J Biol Macromol 123: 322-334, 2019.
37. Li Y, Wang Z, Li J and Sang X: Diallyl disulfide suppresses FOXM1-mediated proliferation and invasion in osteosarcoma by upregulating miR-134. J Cell Biochem: Nov 1, 2018 (Epub ahead of print). doi: 10.1002/jcb.28003.
38. Wang L, Lu J, Zhang H, Lyu X and Sun Z: MicroRNA-876-5p inhibits the progression of glioblastoma multiforme by directly targeting Forkhead box M1. Oncol Rep 41: 702-710, 2019.
39. Chen Q, Zhang J, He Y and Wang Y: hsa_circ_0061140 knockdown reverses FOXM1-mediated cell growth and metastasis in ovarian cancer through miR-370 sponge activity. Mol Ther Nucleic Acids 13: 55-63, 2018.
40. Jin C, Liu Z, Li Y, Bu H, Wang Y, Xu Y, Qiu C, Yan S, Yuan C, Li R, *et al*: PCNA-associated factor P15PAF, targeted by FOXM1, predicts poor prognosis in high-grade serous ovarian cancer patients. Int J Cancer 143: 2973-2984, 2018.
41. Vasudevan HN, Braunstein SE, Phillips JJ, Pekmezci M, Tomlin BA, Wu A, Reis GF, Magill ST, Zhang J, Feng FY, *et al*: Comprehensive molecular profiling identifies FOXM1 as a key transcription factor for meningioma proliferation. Cell Rep 22: 3672-3683, 2018.
42. Yoshida Y, Wang IC, Yoder HM, Davidson NO and Costa RH: The forkhead box M1 transcription factor contributes to the development and growth of mouse colorectal cancer. Gastroenterology 132: 1420-1431, 2007.